IPC EXPO
Technical Conference
San Diego, CA, April 2-7, 2000

Permittivity Measurements of High Dielectric Constant Films at Microwave Frequencies

J. Obrzut and R. Nozaki
NIST, Polymers Division
Gaithersburg, MD 20899-854, USA

Abstract **We have developed a time-domain reflectometry (TDR) technique to measure the dielectric permittivity of high dielectric constant films. The test specimen consists of a planar capacitor terminating coaxial waveguide. The complex permittivity of the dielectric in the frequency domain is obtained from appropriate analysis of the incident and the reflected voltage waves. In order to improve accuracy at higher frequencies, a working equation is proposed to account for propagation in the specimen section. The applicability of the method has been verified at frequencies from 100 MHz to 10 GHz on several polymer composite films, 40 mm to 100 mm thick, having a dielectric constant ranging from 4 to 40. The results obtained in the broad frequency range by using the TDR technique were compared with those obtained from the gap-coupled microstrip resonators at discrete frequencies.**

Keywords **- dielectric permittivity, broadband measurements, coaxial discontinuity, microwave characterization, TDR.**

Introduction

Polymer based high dielectric constant films can be used to construct discrete RLC lumped circuits and de−coupling power planes for wireless communication and high-speed electronics that operate at microwave frequencies. The high dielectric constant of these materials allows multiple wavelengths guided in a small dimension, making them also attractive for highly integrated packaging. In order to develop and successfully commercialize such materials, the industry needs a suitable test method to measure the dielectric permittivity in planar thin film configuration. However, most of the existing microwave methods of permittivity measurement are not feasible for thin films and small dimensions. For example, test procedures utilizing a lumped element are limited to the frequency range below 1 GHz[1] while those based on microwave cavities, or microstrip resonators require rather large samples [2-4]. In the resonant techniques, the radiation losses and non-optimized coupling conditions are common sources of errors in the measured permittivity. Additional difficulties arise from electrical requirements, which for high dielectric constant films can be realized only with tiny patterns and highly conducting metal traces that are hard to fabricate and evaluate. Thus the resonant techniques usually utilize a unique sample configuration useful for certain type of materials at specific frequencies[5-6]. In contrast, time-domain reflectometry (TDR) offers broadband measurements. When compared to other techniques, time-domain reflectometry provides a more intuitive and direct insight into specimen characteristics, which is very convenient in materials characterization and development of new testing procedures. The TDR method has been used to determine an effective dielectric constant of printed circuit board materials by using a co-planar transmission line[7]. In contrast, TDR measurement of complex permittivity is based on analysis of the total reflection pattern produced by the dielectric specimen terminating a coaxial line. This approach has been widely used to characterize the dielectric properties of liquids in several cell configurations[8]. Among them, a lumped capacitance termination corresponds to the smallest cross-section of the specimen, for which approximate expression for the input admittance has been established assuming quasi-static conditions[9]. At higher frequencies thin film specimens require, however, a more accurate solution to account for non-stationary electric fields and wave propagation in the sample section, which has not been previously considered.

In this paper we examined the applicability of the TDR technique to permittivity measurements of high dielectric constant films in the microwave range. We introduced a simplified expression to account for the wave propagation in the sample section, which improved accuracy of measurements at higher frequencies. The results obtained in the broad frequency range by using the TDR technique were

compared with those obtained from the gap-coupled microstrip resonators at discrete frequencies.

Basic Analysis

The experimental arrangement under consideration is shown in Fig. 1. A dielectric film of thickness *t* is placed at the end of the coaxial line of impedance Z_{0l}

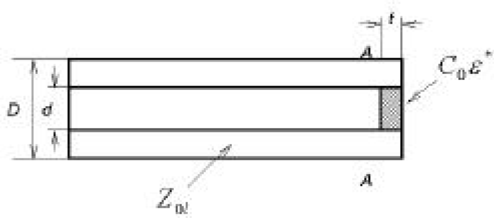

Fig. 1. Sample holder configuration

and length *l*. When a voltage step of amplitude V_i is launched into the line, it is partially reflected back at the discontinuity *A-A*, and then is added to the input step after a delay $\tau_0 = 2l/\upsilon_p$, where υ_p denotes the velocity of propagation. The shape of the reflected wave V_r depends on the nature and magnitude of mismatch between the line impedance Z_{0l} and impedance of the termination. Examples of the load effect on the shape of TDR responses are illustrated in Fig. 2. In Fig. 2a the incident wave is reflected at an open circuit. Since both the incident wave and the reflected wave are in phase, $V_r = V_i$, they combine after the time τ_0 , resulting in the reflected amplitude of $2V_i$. In comparison, the reflected wave at a short

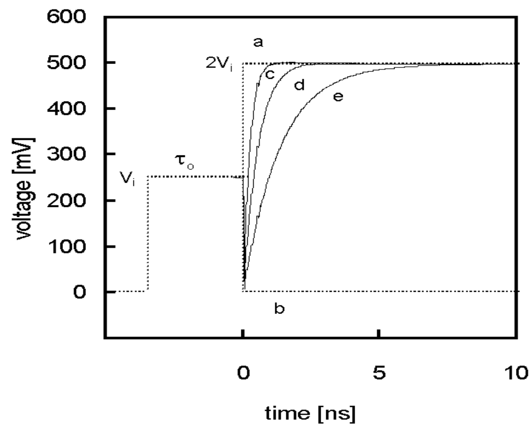

Fig. 2. Dependence of the TDR response on the termination. a – short, b – open, c – 10 μm air-gap, d - 2 μm air-gap, e - 100 μm film having the static dielectric constant

circuit is out of phase by 180° in respect to the incident wave, $V_r = - V_i$, and thus the initial step returns to zero after the time τ_0 , as it is illustrated in Fig. 2b. The TDR response produced by a 250 mV step reflected at air-capacitance having gap of 10 μm and 2 μm, is shown in plots c and d of Fig. 2 respectively. Example response from a 100 μm thick dispersive film, having at 3 GHz a dielectric constant of 36 is shown in Fig. 2e.

In all three illustrations where the line is terminated with a lumped capacitance, the resulting reflection exhibits a positive going transfer that is exponential in time. The electrical circuit corresponds to a complex shunt R-C termination for which the transient voltage can be described by equation (1).

$$V_r(\tau) = V_i\ [(1+\frac{R-Z_{0l}}{R+Z_{0l}})(1-\exp(-\frac{\tau}{T}))] \quad (1)$$

where $T = \frac{Z_{0l}R}{Z_{0l}+R}C$ is the relaxation charging time.

For simplicity, the time parameter in equation (1) is chosen to be zero when the reflected wave arrives back to the detector, τ at $\tau_0 = 0$. It is seen that at time zero the R-C load depends on C as a short circuit. Then the voltage builds up across the capacitance increasing its impedance until it effectively becomes an open circuit. From equation (1) the total voltage at $\tau = \infty$ is $(1+(R - Z_{0l})/(R+ Z_{0l}))\ V_i$, which approaches $2V_i$ when R becomes infinitely large. This corresponds to a dielectric with negligible loss, such as an air-gap terminating the transmission line as shown in Fig. 2, plots c and d.

The circuit expressions such as (1), are better suited for calculation of the expected behavior for a given dielectric rather than for evaluation of permittivity from the experimental voltage waves. In fact, an explicit solution for permittivity cannot be obtained even for the simplest dielectric relaxation mechanism since it is simultaneously entangled with reflection coefficient and propagation functions. Thus only approximate solutions are possible. A time dependent voltage across the sample, $V(\tau)$, can be related to a time dependent charge and the geometric capacitance through an appropriate response function which links the reflected wave with the dielectric permittivity ε* of the specimen. Evaluation of ε* from the observed reflected voltage wave, V_r, involves Laplace transformation of the response function obtained in the time domain and the propagation equation for the

coaxial line, with appropriate boundary conditions. Usually, a thin film capacitance at the end of the coaxial line has been treated as a primary capacitance with a fringing field capacitance without electrical length[10]. Such treatment becomes inaccurate at short times (high frequencies) for a finite film, which represents a radial waveguide of cylindrical cross-section. The incident pulse through the coaxial line is partially reflected at the discountinuity while some portion of it propagates inside the capacitance perpendicularly to the initial direction. The reflection-transmission repeats at the other edge of the capacitance where the residual wave is being transmitted back to the coaxial line with the propagation delay associated with single passing through the specimen section. This is equivalent to a capacitor inserted between two matched lines. The input admittance of such structure can be described as follows[10]:

$$Y_{in} = j\mathbf{w}\, C_0 \mathbf{e}_r^* (x \cot x)^{-1} \qquad (2)$$

where $x = \frac{\mathbf{w} d}{2c}\sqrt{\mathbf{e}_r^*}$ accounts for the propagation inside the capacitor along its diameter d , $\mathbf{e}_r^* = \mathbf{e}' + j\mathbf{e}''$ is the relative complex permittivity of the specimen, $\mathbf{w}$ is an angular frequency, c is the velocity of propagation in vacuum, and C_0 represents a total geometric capacitance of the line given by a sum of the primary, C_p, and the fringing field capacitance, C_f, respectively[8]; $C_0 = C_p + C_f$.

On the other hand, the input admittance is given by using measurable TDR waves:

$$Y_{in} = G_{0l}\frac{V_i(j\mathbf{w}) - V_r(j\mathbf{w})}{V_i(j\mathbf{w}) + V_r(j\mathbf{w})} \qquad (3)$$

where $V_i(j\mathbf{w})$ and $V_r(j\mathbf{w})$ are the Laplace transforms of the incident and the reflected waves, and G_{0l} is the characteristic conductance of the coaxial line.

By combining equations (2) and (3) we obtain expression (4) for $\mathbf{e}^*$ as a function of measurable incident and reflected waves, V_i and V_r, that are referenced at the time $\mathbf{t}_0$ as it is shown in Fig. 2:

$$\mathbf{e}^* = \frac{c}{j\mathbf{w}(gd)}\frac{V_i(j\mathbf{w}) - V_r(j\mathbf{w})}{V_i(j\mathbf{w}) + V_r(j\mathbf{w})} f \qquad (4)$$

where:

$gd = C_p G_{0v} / (\mathbf{e}_0 G_{0l})$ accounts for the cell constant, $f = x \cot x$, $\mathbf{e}_0$ is the dielectric constant of vacuum, $G_{0v} = 1/376.73$ $[1/\Omega]$ is the characteristic conductance of vacuum and G_{0l} is the characteristic conductance of the line. It is convenient to avoid using the input step wave V_i in (4), which introduces some, difficult to account for numerical errors due to finite rise time and limited flatness of the generated step voltage. Instead, reflection measurements on a standard specimen with known permittivity can be utilized. For two specimens, one with known permittivity $\mathbf{e}_s^*$, and the other with unknown permittivity $\mathbf{e}_x^*$, expression (4) can be rewritten as follows:

$$\mathbf{e}_x^* = \frac{c}{j\mathbf{w}(gd)_x}\frac{R + P_s}{RP_s + 1} f_x \qquad (5)$$

where parameters R and P_s are given as: $R = \frac{V_s(j\mathbf{w}) - V_x(j\mathbf{w})}{V_s(j\mathbf{w}) + V_x(j\mathbf{w})}$, $P_s = \frac{j\mathbf{w}(gd)_s}{cf_s}\mathbf{e}_s^*$, and $f_{x,s} = x_{x,s} \cot x_{x,s}$ respectively.

In comparison to equation (4) equation (5) does not include the Laplace transform of the incident wave, which simplifies the computational procedure. In addition, measurements against a standard dielectric specimen minimize the systematic uncertainty.

Experimental

The test methodology has been examined experimentally using a dielectric test fixture constructed from two altered APC-7 to APC-3.5 adapters shown in Fig. 3. In section A, the inner conductor was replaced with a shorting piston fitting precisely into the 7 mm diameter of the adapter. The vertical position of the piston could be controlled with a micrometer assembled on the 3.5 mm side of the APC adapter. In the air portion of section B, the center conductor was replaced with a fixed 3.0 mm diameter pin, machined precisely to achieve flat and parallel contact with the shorting piston in section A. Using a differential micrometer, for example Newport Model DM-13 or similar, the distance between the pin and the piston can be adjusted from 0 µm to 200 µm with 0.1 µm resolution. Thus the fixture can be used as an electrical short, standard air-gap capacitor, or sample holder for low and high

dielectric constant films. In comparison to other fixtures that utilize coaxial connectors or coupling probes, this compact test fixture minimizes radiation losses, coupling errors and errors caused by inductive components.

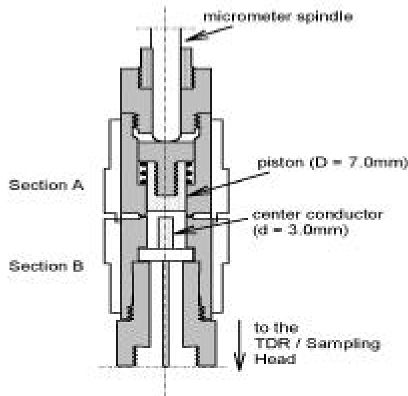

Fig. 3. Test Fixture

The TDR measurements were carried out using a Tektronix 11802 Digital Sampling Oscilloscope equipped with a TEK SD-24 TDR/Sampling Head. A VEE 5.0 software platform from Hewlett Packard was used for acquisition and processing of the data. Waveforms were captured in a 10 ns window typically containing 1024 data points with a resolution of 2.5 ps. High dielectric constant materials were obtained from the NCMS Embedded Capacitance Project[11]. The TDR test specimens were prepared from copper-cladded dielectric films by defining 3 mm diameter metal electrodes using photolithography. A similar procedure was used to fabricate microstrip resonators, which were defined along with the corresponding co-planar terminations as a two-level circuitry. The microstrip dimensions and coupling conditions were optimized to avoid overlapping of higher order modes and to achieve a low loading level at the resonance[12]. Resonant frequencies were detected using a HP 8720D Network Analyzer and Cascade ACP-40-W-GSG probes.

Results and Discussion

The results of the dielectric constant measurements are illustrated in Fig.s 4 and 5. Fig. 4a shows the dielectric constant, $\varepsilon_a^{'}$, of a 2 µm air-gap measured by the TDR from 100 MHz to about 15 GHz using a

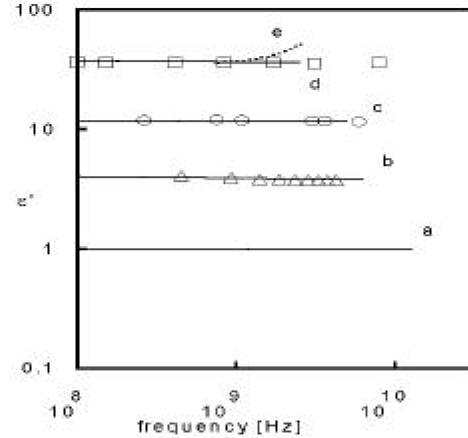

Fig. 4. Dielectric constant, ε' of film specimens measured by the TDR method (lines) is compared with results obtained from the microstrip resonators at discrete frequencies (points). (a -): 2 µm air-gap; (b – triangles): 50 µm thick film with the static dielectric constant ε'_{DC} of 4; (c - circles): 40 µm thick film ε'_{DC} of 12; (d - squares): 100 µm thick film ε'_{DC} of 38; (e –): thin film approximation for the specimen (d).

10 µm air-gap as a standard. In the frequency range of up to 10 GHz the relative uncertainty, $(\Delta\varepsilon_a^{'})/\varepsilon_a^{'}$, determined as a deviation from the standard value is below 2 %. At higher frequencies, above 10 GHz the uncertainty increases to about 8 % due to

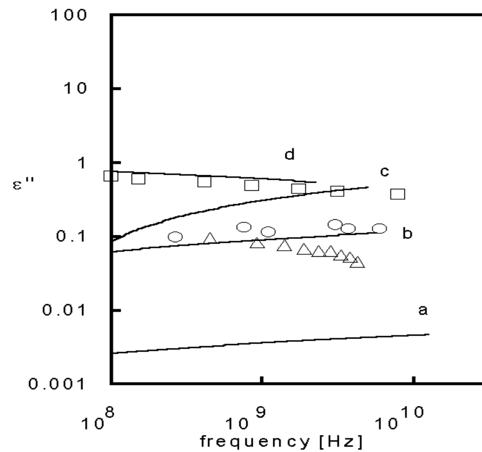

Fig. 5. Dielectric loss, ε'' of film specimens measured by the TDR method (lines) is compared with results obtained from the microstrip resonators at discrete frequencies (points). (a -): 2 µm air-gap; (b – triangles): 50 µm thick film with the static dielectric constant ε'_{DC} of 4; (c - circles): 40 µm thick film ε'_{DC} of 12; (d - squares): 100 µm thick film ε'_{DC} of 40.

irreproducible behavior of the test fixture that could not be compensated by the short calibration. Fig. 5a shows the corresponding results of the dielectric loss measurements, e''_a. The combined uncertainty for the dielectric loss, $\Delta e''_a$, is estimated to be less than 0.01 in the same frequency range.

Our procedure fails to provide meaningful data above 15 GHz. The difficulties in that range originate from the instrumental limits in the voltage step generation, timing, and waveform detection. The experimental error in permittivity measurements for an unknown specimen can be minimized to the level indicated above for the air-gap if the TDR response of the unknown specimen follows that of the standard. In practice, the measured waveform differs from that of the standard and the uncertainty in the measured permittivity is larger due to uncompensated electrical noise errors such as the time and the amplitude jitter, and errors resulting from the time-to-frequency conversion. It has been determined that the combined uncertainty, $\Delta e''_x$, for an unknown specimen can be evaluated using the relaxation charging time, T (see equation 1), as an indicator of deviation from the standard behavior. If the value of complex permittivity for the standard sample has uncertainty Δe^*_s, the uncertainty Δe^*_x for the unknown specimen can be obtain from expression (6).

$$\Delta e^*_x = \Delta e^*_s \times 10^{|\log(T_X/T_S)|} \qquad (6)$$

where T_x is the relaxation charging time for the unknown sample and T_s denotes the relaxation charging time for the standard.

The dielectric permittivity results for an FR4-based epoxy resin film, and two $BaTiO_3$ filled high dielectric composite films are shown in Fig. 4b, 4c and 4d. At 3 GHz the permittivity of the materials (b), (c) and (d) is: e^*_b = (3.8 + j0.08), e^*_c = (11.8 + j0.24) and e^*_d = (38.1 + j0.81) respectively. The relative uncertainty of measurements obtained from equation (6) for the specimens (b) is 2% , for (c) is within 10 %, and for the specimen (d) the uncertainty is within 12 %. It is seen in Fig.s 4 and 5 that the TDR results agree rather well with the permittivity values determined by the resonance method at the discrete frequencies.

The upper frequency limit in the TDR measurements shown in Fig. 4, is related to a half-wavelength resonance conditions in the dielectric film. The conditions for the resonant frequency can be obtained from equation (2) by noting that the first zero of *x cot (x)* occurs at $x = \pi/2$. Therefore, the resonant frequency is $f_r = c/(2d$ **Öe¢**, where d is the 3.0 mm diameter of the film specimen rather than the film thickness. Thus, for the film with the dielectric constant of 38 the first resonant frequency f_r is about to about 8 GHz. The multiple reflection pattern due to propagation in the higher dielectric constant specimens has been observed directly on the TDR waveform shown in Fig. 6.

The time between consecutive reflections is about 60 ps, which for the dielectric constant of 38 corresponds to the propagation length of about 3 mm, and thus, coincides with the diameter of the specimen. This experimental result reaffirms the correctness of the fundamental approach and simplifications behind the working equation (4). In comparison to the thin film approximation, the

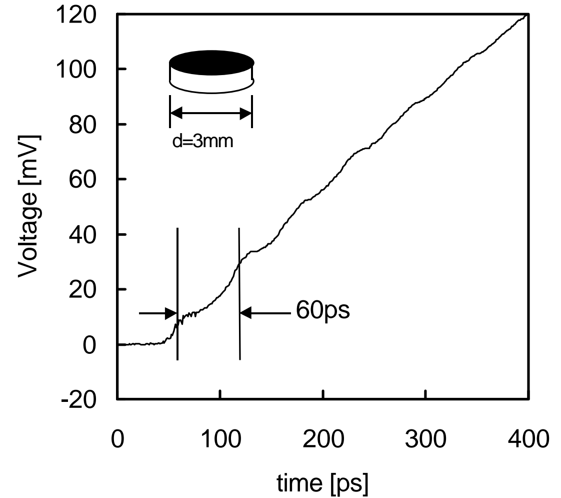

Fig. 6. Propagation delay of 60 ps is superimposed on the TDR waveform of the film specimen having diameter of 3 mm and the value of the dielectric constant of 38.

presented methodology provides more accurate results at higher frequencies, especially for high dielectric constant films (see Fig. 4e). The thin film configuration does not compromise the loss measurements since the propagation length is independent of the specimen thickness. However, the upper frequency range is limited by a singular behavior of equation 4 near a quarter-wavelength resonance, due to wave propagation in the specimen section. For a given dielectric film the upper frequency limit can be increased by decreasing the propagation length using a smaller diameter fixture,

for example the 3.5 mm standard instead of the 7.0 mm.

Conclusion

A time-domain reflectometry technique has been developed to measure permittivity of dielectric films in the broad frequency range including the microwave. The technique can utilize an air-gap, or any dielectric film of known permittivity as a reference to minimize the systematic uncertainty. In order to account for wave propagation in the specimen section, a working equation has been delivered to account for the propagation in the specimen section. In comparison to the previously developed thin film approximations, the presented methodology provides more accurate results at higher frequencies, especially for high dielectric constant films.The technique has been evaluated at frequencies from 100 MHz to 10 GHz using several polymer composite films, 40 μm to 100 μm thick, having the dielectric constant ranging from 4 to 40. The results obtained in the broad frequency range by the TDR compared well with those obtained from the gap-coupled microstrip resonators at discrete frequencies.

Acknowledgment

This work was supported in part by the NIST Advanced Technology Program.

Disclaimer

Certain materials and equipment identified in this manuscript are solely for specifying the experimental procedures and do not imply endorsement by NIST or that they are necessary the best for these purposes.

References

1. ASTM D150, D669, IPC TM-650, 2.5.5.1-9, "Permittivity (dielectric constant) and loss tangent (dissipation factor) of insulating materials", Rev. 5/86.
2. ASTM 3380, IPC TM-650, 2.5.5.5, "Stripline test for complex permittivity of circuit board materials to 14 GHz", Rev. 5/97.
3. M. A. Saed, "Measurement of the Complex Permittivity of Low- Loss Planar Microwave Substrates using Aperture-Coupled Microstrip Resonators", IEEE Trans. Microwave Theory Meas., Vol. MTT 41, pp. 1343-1348, 1993.
4. Y. Kantor, "Dilelectric constant measurements using printed circuit techniques at microwave frequencies", Proceedings of the Mediterranean Electrotechnical Conference - MELECON. Part 1 (of 2) May 18-20 1998, Tel-Aviv, Israel, Vol. 1 pp. 101-105, 1998, Sponsored by: IEEE Piscataway NJ USA.
5. C. D. Gupta, " A new microwave method of measuring complex dielectric constant of high-permittivity thin films", IEEE Trans. Instr. Meas., Vol. IM 24, pp. 61-65, 1975.
6. D. Galt and J. C. Price, "Ferroelectric thin film characterization using superconducting microstrip resonators", IEEE Trans. Appl. Supercond., Vol. 5, pp. 2575-2578, 1995.
7. N. G. Paulter, "A fast and accurate method for measuring the dielectric constant of printed wiring board materials", IEEE Trans, Comp., Pack., Manuf., Techn., Vol. 19, pp. 214-225, 1996.
8. M. A. Stuchly and S. S. Stuchly "Coaxial-line-reflection methods for measuring dielectric properties of biological substances at radio and microwave frequencies- a review" IEEE Trans. Instr. Meas., Vol. IM 29, pp. 176-183, 1980.
9. M. F. Iskander and S.S Stuchly, "A time domain technique for measurements of the dielectric properties of biological substances", IEEE Trans. Instr. Meas., Vol. IM 21, pp. 425-429, 1972.
10. R. Nozaki and T. K. Bose, "Broadband complex permittivity measurements by time-domain spectroscopy" IEEE Trans. Instr, Meas., Vol. 39, pp. 945 – 951 1990.
11. "Embedded Capacitance Workshop" NCMS, February 28-29, 2000, Tempe AZ.
12. K. C. Gupta, R. Garg, I. Bahl and P. Bhartia, Microstrip Lines and Slotlines, Artech House, Boston, 1996.